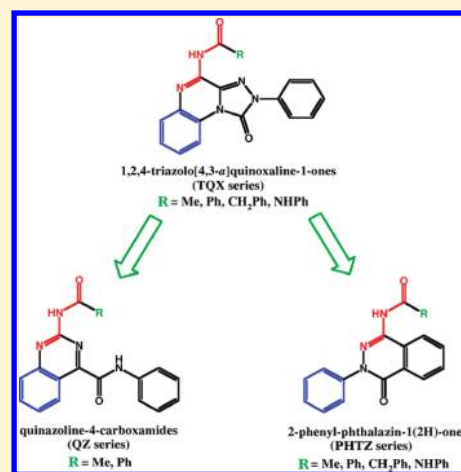# The Identification of the 2-Phenylphthalazin-1(2*H*)-one Scaffold as a New Decorable Core Skeleton for the Design of Potent and Selective Human A₃ Adenosine Receptor Antagonists

Daniela Poli,[†] Daniela Catarzi,*,[†] Vittoria Colotta,[†] Flavia Varano,[†] Guido Filacchioni,[†] Simona Daniele,[‡] Letizia Trincavelli,[‡] Claudia Martini,[‡] Silvia Paoletta,[§] and Stefano Moro*,[§]

[†]Dipartimento di Scienze Farmaceutiche, Università degli Studi di Firenze, Polo Scientifico, Via U. Schiff, 6-50019 Sesto Fiorentino (Firenze), Italy

[‡]Dipartimento di Psichiatria, Neurobiologia, Farmacologia e Biotecnologie, Università degli Studi di Pisa, Via Bonanno, 6-50126 Pisa, Italy

[§]Molecular Modeling Section (MMS), Dipartimento di Scienze Farmaceutiche, Università degli Studi di Padova, via Marzolo 5, I-35131 Padova, Italy

S *Supporting Information*

ABSTRACT: Following a molecular simplification approach, we have identified the 2-phenylphthalazin-1(2*H*)-one (PHTZ) ring system as a new decorable core skeleton for the design of novel hA₃ adenosine receptor (AR) antagonists. Interest for this new series was driven by the structural similarity between the PHTZ skeleton and both the 2-aryl-1,2,4-triazolo[4,3-*a*]quinoxalin-1-one (TQX) and the 4-carboxamido-quinazoline (QZ) scaffolds extensively investigated in our previously reported studies. Our attention was focused at position 4 of the phthalazine nucleus where different amido and ureido moieties were introduced (compounds **2−20**). Some of the new PHTZ compounds showed high hA₃ AR affinity and selectivity, the 2,5-dimethoxyphenylphthalazin-1(2*H*)-one **18** being the most potent and selective hA₃ AR antagonist among this series (K_i = 0.776 nM; hA₁/hA₃ and hA₂ₐ/hA₃ > 12000). Molecular docking studies on the PHTZ derivatives revealed for these compounds a binding mode similar to that of the previously reported TQX and QZ series, as was expected from the simplification approach.

1,2,4-triazolo[4,3-*a*]quinoxaline-1-ones
(TQX series)
R = Me, Ph, CH₂Ph, NHPh

quinazoline-4-carboxamides
(QZ series)
R = Me, Ph

2-phenyl-phthalazin-1(2H)-ones
(PHTZ series)
R = Me, Ph, CH₂Ph, NHPh

■ INTRODUCTION

The autacoid adenosine plays a pivotal role in a large variety of physiological and pathophysiological processes both in the central nervous system (CNS) and in the periphery. Adenosine is physiologically present in the extracellular fluid and exerts its effects through activation of four cell surface receptor subtypes termed A₁, A₂ₐ, A₂ᵦ, and A₃, which belong to the superfamily of G protein-coupled receptors (GPCRs).[1,2] Adenosine receptors (ARs) are widely distributed in the body and are expressed with different density in the various tissues. The classical transduction intracellular pathways associated with AR stimulation are inhibition, via $G_{i/o}$ protein (A₁ and A₃ subtypes), or activation, via G_s protein (A₂ₐ and A₂ᵦ receptors), of adenylate cyclase (AC).[1] More recently, other second messenger systems, such as phospholipase C[3] or potassium[4] and calcium channels,[4,5] have been described as relevant for AR signaling.

Under normoxic conditions, adenosine modulates the activity of the nervous system through stimulation of high affinity A₁ and A₂ₐ receptors, which are highly expressed in the brain. Although the activation of A₁ and A₂ₐ subtypes influences neurotransmission in

an opposite manner (through inhibition and stimulation, respectively), the global effect of the fine-tuner adenosine is inhibitory. The A₂ᵦ and A₃ subtypes are low affinity ARs and might be outstanding in pathological states. In fact, it is well-known that under physiological conditions, A₃ receptors do not have relevant effects on neurotransmission, while no data are available on the role of the A₂ᵦ subtype.[6,7]

A large body of experimental evidence has pointed out the A₁ and A₂ₐ receptor-mediated neuroprotective effects. Activation of A₁ AR leads to the minimization of the toxic effect promoted by excitatory neurotransmitters, while the A₂ₐ subtype mediates the activation of endogenous neuroprotective mechanisms.[7,8]

More recently, also the involvement of A₃ AR in neuroprotection has been proposed.[7,9−12] However, up to now, it is not clear which is the real role of this receptor in ischemic conditions: The mixed A₃-mediated protective/damaging effect is still enigmatic and has to be clarified.[5,7,9,13] This dichotomic behavior of the A₃
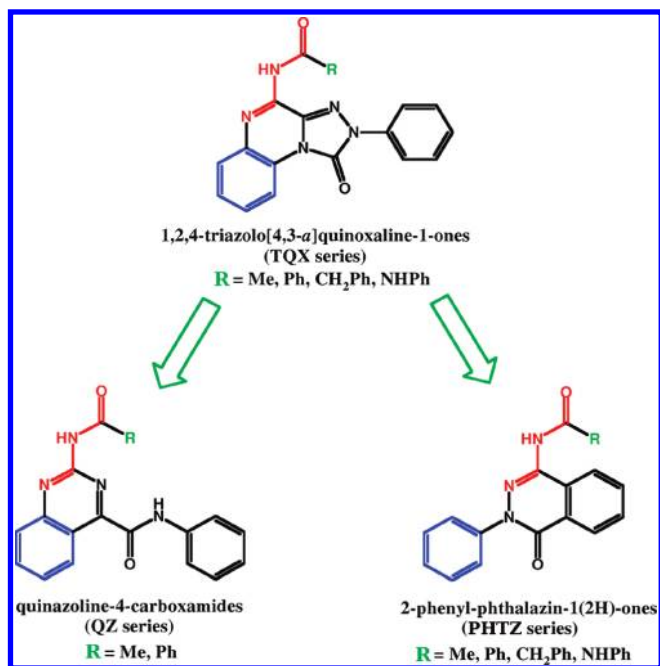
Figure 1. Simplification approach: from the TQX series to the QZ series and to the herein reported 2-phenylphthalazin-1(2H)-one derivatives (PHTZ series). Colors identify important conserved groups in different series.

subtype has been highlighted also in other different pathological conditions such as cancer and inflammation, where this receptor seems to mediate contrasting effects.[9] Thus, numerous A_3 AR agonists and antagonists have been investigated for their potential therapeutic applications[7,9−12,14−17] and to shed light on which could be the best choice for a given disease. It is easy to understand why we have directed our efforts in this intriguing direction and why, in the past few years, our attention has been focused on the development of adenosine A_3 receptor antagonists. Our research has led to the discovery of many tricyclic compounds belonging to strictly correlated classes of nitrogen-containing heterocycles and showing high affinity and selectivity toward adenosine A_3 receptor.[12,18−27] Besides their remarkable pharmacodynamic profiles, a favorable spectrum of pharmacokinetic properties as well as the straightforwardness of their synthetic pathway have to be considered as essential requirements for any drug candidate.

Indeed, our previously reported studies confirmed that structural simplification can represent a drug design strategy to shorten synthetic routes while keeping or enhancing the biological activity of the original candidate.[28,29] In particular, we have already reported that the 2-aryl-1,2,4-triazolo[4,3-a]quinoxalin-1-one (TQX)[18,20,21,24,25] series can be simplified into new easily synthesizable 4-carboxamido-quinazoline (QZ) derivatives endowed with high affinity and selectivity toward hA_3 AR.[28] In our investigations, many other bicyclic heteroaromatic systems, containing those structural features essential to guarantee an efficient ligand−receptor recognition, have been taken into consideration as a possible core skeleton for the design of novel hA_3 AR antagonists. Among them, our attention has been caught by the phthalazin-1(2H)-one (PHTZ) ring system that has not yet been considered as a suitable scaffold to obtain AR antagonists.

Our interest for this new series of PHTZ analogues was also driven by the structure similarity between the phthalazin-1(2H)-

one skeleton and both TQX and QZ scaffolds extensively investigated in our previously reported studies[21,24,25,28] (Figure 1). In this first part of our work, we focused our attention at position 4 of the phthalazine ring system, where differently substituted amido and ureido moieties were introduced (compounds 2−20, Table 1). In contrast, the 2-phenyl-substituent was held constant. Interestingly, also, an in silico receptor-driven analysis on all the three (TQX, QZ, and PHTZ) series led to the identification of converging ligand−receptor binding requirements, which we consider as essential features for profitable hA_3 receptor−antagonist recognition.

■ CHEMISTRY

The 4-substituted-2-phenylphthalazin-1(2H)-one derivatives 2−20 and the parent 4-amino compound 1 were prepared following the synthetic pathway depicted in Scheme 1. By reacting phthalic anhydride with an excess of phenylhydrazine, the 4-hydroxy-2-phenylphthalazin-1(2H)-one 21[30,31] was obtained, which was treated with $POCl_3$ to yield the corresponding 4-chloro derivative 22.[32] Subsequently, reaction of 22 with hydrazine sulfate in anhydrous hydrazine gave the 4-hydrazino compound 23,[32] which was reduced with hydrogen, in the

Scheme 1[a]
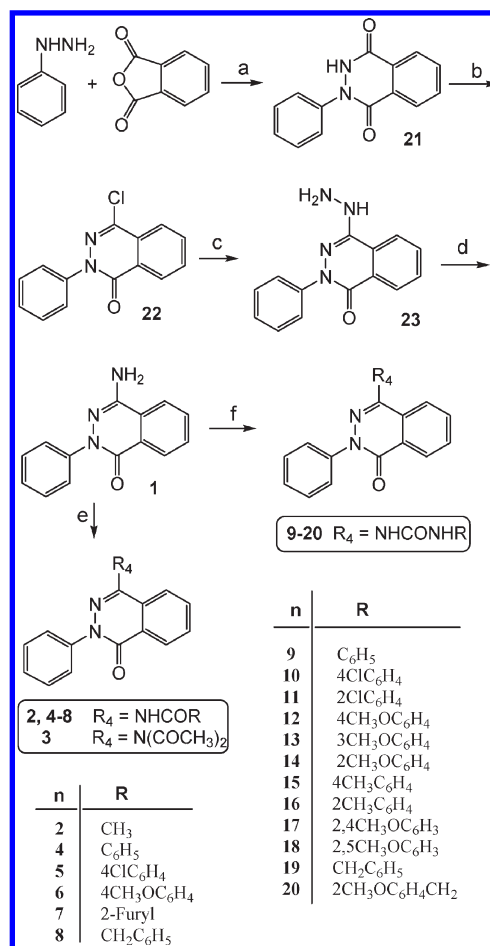
[a] Reagents and Conditions: (a) 10% HCl; (b) $POCl_3$; (c) $NH_2NH_2xH_2SO_4$, NH_2NH_2, ethylene glycol; (d) H_2, Raney-Nickel, EtOH; (e) RCOCl, pyridine, THF; (f) RNCO, CH_2Cl_2 or THF.

presence of Raney nickel as catalyst, to the corresponding 4-amino-2-phenylphthalazin-1(2H)-one **1** with good yield.

The 4-aroylamino-2-phenylphthalazin-1(2H)-ones **2** and **4**−**8** were obtained by reacting **1** with the suitable aroyl chloride in the presence of pyridine. In the preparation of the 4-acetylamino compound **2**, treatment of **1** with acetyl chloride also gave the corresponding diacetylamino derivative **3**. Reaction of **1** with the appropriate aryl or alkyl isocyanate produced the targeted 4-ureido compounds **9**−**20**.

■ PHARMACOLOGY

The newly 4-substituted phthalazine derivatives **2**−**20** and the parent **1** (Table 1) were tested for their ability to displace [^{125}I]N^6-(4-amino-3-iodobenzyl)-5′-(N-methylcarbamoyl)adenosine ([^{125}I]AB-MECA) from cloned hA$_3$ receptor stably expressed in Chinese hamster ovary (CHO) cells. Subsequently, all compounds were evaluated for their ability to displace [^{3}H]8-cyclopentyl-1,3-dipropylxantine ([^{3}H]DPCPX) from cloned hA$_1$ ARs and [^{3}H]5′-(N-ethylcarboxamido)adenosine ([^{3}H]NECA) from cloned hA$_{2A}$ ARs, to establish their A$_3$ versus A$_1$ and versus A$_{2A}$ selectivity.

Moreover, some selected compounds (**12**−**14**, **18**, and **19**) were tested at the hA$_{2B}$ subtype by measuring their inhibitory effect on NECA-stimulated cyclic adenosine monophosphate (cAMP) levels in CHO cells stably transfected with the hA$_{2B}$ AR (Table 2). To evaluate their hA$_3$ AR antagonistic effect, the same compounds were tested for their ability to counteract the NECA-mediated inhibition of cAMP accumulation in CHO cells stably expressing hA$_3$ AR (Table 2).

The binding data of derivatives **1**−**20** are shown in Table 1 together with those of **A** (1,2-dihydro-2-phenyl-4-phenylureido-1,2,4-triazolo[4,3-a]quinoxalin-1-one)[18] and **B** (2-benzoylaminoquinazoline-4-carboxyanilide),[28] selected as reference compounds of the TQX and QZ series, respectively.

■ MOLECULAR MODELING

To explain the observed structure−affinity relationships (SARs) and the selectivity profile of these new 2-phenylphthalazin-1(2H)-one derivatives in comparison with the previously reported TQX and QZ series,[21,24,25,28] a receptor-driven molecular modeling investigation, based on a lately proposed model of the hA$_3$ receptor derived from the crystallographic structure of hA$_{2A}$ AR, was also performed in this study.

In fact, the recently published crystallographic structure of hA$_{2A}$ AR, in complex with the high affinity antagonist ZM241385 {4-(2-[7-amino-2-(2-furyl)[1,2,4]-triazolo[2,3-a][1,3,5]triazin-5-ylamino]ethyl)phenol} (PDB code: 3EML),[33] provides a new alternative template to perform homology modeling of other GPCRs and in particular of ARs. Therefore, a homology model of the hA$_3$ receptor based on the crystal structure of the hA$_{2A}$ receptor was constructed as previously described[29,34] (methodological details are summarized in the Experimental Section).

Then, in the process of selecting a reliable docking protocol to be employed in the following docking studies of the new PHTZ derivatives, we evaluated the ability of different docking softwares to reproduce the crystallographic pose of ZM241385 inside the binding cavity of hA$_{2A}$ receptor. As reported in the Experimental Section, among the four different types of programs used to calibrate our docking protocol, the Gold program was finally chosen since it showed the best performance with regards to the

calculated root-mean-square deviation (rmsd) values relative to the crystallographic pose of ZM241385.[29]

Consequently, on the basis of the selected docking protocol, we performed docking simulations to identify the hypothetical binding modes of the newly synthesized 2-phenylphthalazin-1(2H)-one derivatives and of two previously reported TQX and QZ derivatives, inside the hA$_3$ and hA$_{2A}$ ARs.

Finally, to analyze the possible ligand−receptor recognition mechanism in a more quantitative way, the individual electrostatic ($\Delta E_{\text{int}}^{\text{el}}$) and hydrophobic ($\Delta E_{\text{int}}^{\text{hyd}}$) contributions of each receptor residue to the interaction energy (ΔE_{int}) were calculated for all of the selected binding poses (see the Experimental Section for more details).
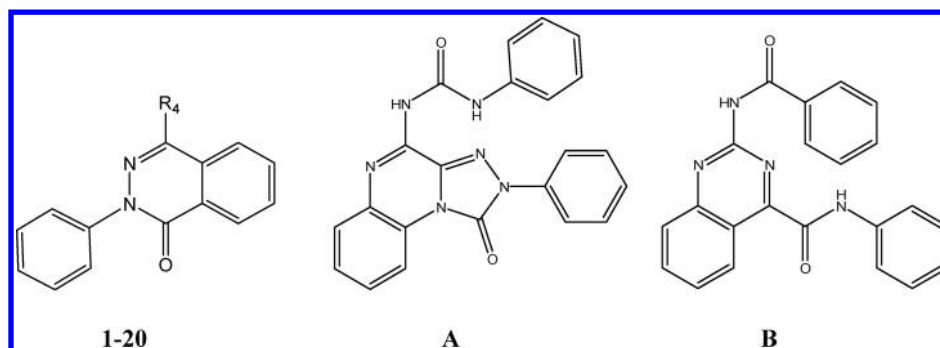
■ RESULTS AND DISCUSSION

Examining the binding results reported in Table 1, it appears that we have identified some new potent and selective adenosine hA$_3$ receptor antagonists belonging to the 2-phenylphtalazin-1(2H)-one series. In particular, it has to be noted that compounds **12**−**14**, **18**, and **19** bearing a methoxyphenyl- or a benzyl-substituted ureido moiety at position 4 are those endowed with high affinity and also selectivity toward the hA$_3$ receptor, as they are on the whole unable to bind at all the others ARs. These preliminary results indicate that the 2-phenylphtalazin-1(2H)-one moiety is a versatile tool for the design of new potent and selective hA$_3$ AR antagonists. However, it is rather evident that clear and robust SARs can be difficult to obtain.

To start in, the binding affinity at the hA$_3$ receptor of the 4-amino-2-phenylphtalazin-1(2H)-one **1** (hA$_3$ I = 8%) was very discouraging in particular because it was not in line with that of the 4-amino-2-phenyl-1,2,4-triazolo[4,3-a]quinoxalin-1-one (hA$_3$ K_i = 490 nM)[18] or the 2-aminoquinazoline-4-carboxyanilide (hA$_3$ K_i = 350 nM)[28] belonging to the reference TQX and QZ series, respectively.

Despite this unfavorable starting point and on the basis of the SARs derived from both TQX and QZ hA$_3$ antagonists, a series of 4-amido- (**2**−**8**) and 4-ureido-derivatives (**9**−**20**) were synthesized starting from the 4-amino intermediate **1**. All of the 4-amido compounds, including alkyl- (**2** and **3**), aryl- (**4**−**7**), and also arylalkyl-substituted (**8**), were inactive with the only exception being the 4-phenylamido derivative **4** that showed a K_i value of 1100 nM at the hA$_3$ AR. Very interestingly, replacement of the phenylamido- (**4**) with the phenylureido moiety (**9**) at the 4-position provided an appreciable increase of receptor affinity. In fact, the 4-phenylureido derivative **9** was about 6-fold more active (hA$_3$ K_i = 178.4 nM) than its amido analogue **4**. As previously described for other ureido-related hA$_3$ antagonists,[35] the urea moiety contributes to the observed large differences among the hA$_3$ binding affinities of these derivatives. Thus, the presence of a second NH group able to reinforce the hydrogen bond network within the putative transmembrane (TM) binding cavity appears to be primarily responsible for the ameliorating effect of the receptor−antagonist recognition.

Starting from the encouraging hA$_3$ binding data of the 4-phenylureido compound **9**, we decided to explore the role of a substituted phenyl ring at the level of the 4-ureido moiety by introducing groups with different electronic and lipophilic properties at position ortho, meta, or para. Insertion of the electron-withdrawing and lipophilic chloro atom at position para or ortho produced, respectively, a total loss (compound **10**) or a dramatic reduction (compound **11**) of receptor affinity at the hA$_3$ subtype.

Table 1. Binding Affinity (K_i) of 4-Substituted 2-Phenylphtalazin-1(2H)-one Derivatives 1−20 and of Reference Compounds A and B, of the TQX and QZ series, at Human A$_3$, A$_1$, and A$_{2A}$ ARs

compd	R$_4$	K_i (nM) or I%[a]		
		hA$_3$[b]	hA$_1$[c]	hA$_{2A}$[d]
1	NH$_2$	8%	24%	45%
2	NHCOCH$_3$	0%	52%	14%
3	N(COCH$_3$)$_2$	0%	47%	10%
4	NHCOC$_6$H$_5$	1100 ± 100	44%	35%
5	NHCOC$_6$H$_4$-4-Cl	17%	26%	17%
6	NHCOC$_6$H$_4$-4-OCH$_3$	10%	0%	17%
7	NHCO(furan-2-yl)	8%	23%	41%
8	NHCOCH$_2$C$_6$H$_5$	28%	23%	4%
9	NHCONHC$_6$H$_5$	178.4 ± 17	44%	42%
10	NHCONHC$_6$H$_4$-4-Cl	13%	10%	9%
11	NHCONHC$_6$H$_4$-2-Cl	49%	0%	3%
12	NHCONHC$_6$H$_4$-4-OCH$_3$	60.6 ± 6.2	4%	51%
13	NHCONHC$_6$H$_4$-3-OCH$_3$	9.75 ± 0.25	45%	28%
14	NHCONHC$_6$H$_4$-2-OCH$_3$	8.9 ± 1	0%	17%
15	NHCONHC$_6$H$_4$-4-CH$_3$	45%	29%	0%
16	NHCONHC$_6$H$_4$-2-CH$_3$	22%	20%	28%
17	NHCONHC$_6$H$_3$-2,4-OCH$_3$	33%	29%	33%
18	NHCONHC$_6$H$_3$-2,5-OCH$_3$	0.776 ± 0.037	0%	19%
19	NHCONHCH$_2$C$_6$H$_5$	29.6 ± 3	20%	23%
20	NHCONHCH$_2$C$_6$H$_4$-2-OCH$_3$	274.2 ± 26	28%	28%
A[e]		276 ± 21	50.8 ± 4.2[f]	2300 ± 291[f]
B[g]		182 ± 10	7%	10%

[a] The K_i values are means ± SEMs of four separate assays, each performed in triplicate. [b] Displacement of specific [125I]AB-MECA binding at hA$_3$ receptors expressed in CHO cells or percentage of inhibition (I%) of specific binding at 1 μM. [c] Displacement of specific [3H]DPCPX at hA$_1$ receptors expressed in CHO cells or percentage of inhibition (I%) of specific binding at 10 μM concentration. [d] Displacement of specific [3H]NECA binding at hA$_{2A}$ receptors expressed in CHO cells or percentage of inhibition (I%) of specific binding at 10 μM concentration. [e] Ref 18. [f] Displacement of specific [3H]CHA and [3H]CGS21680 binding at A$_1$ and A$_{2A}$ receptors, respectively, in bovine brain membranes. [g] Ref 28.

The strong electron-donating methoxy group was then introduced on the targeted 4-phenylureido moiety leading to the para-substituted compound 12, which was shown to be highly potent at the adenosine hA$_3$ receptor subtype (hA$_3$ K_i = 60.6 nM). Next, the *para*-methoxy substituent of 12 was moved to position meta and ortho to evaluate whether this shift could further optimize the anchoring at the hA$_3$ receptor site. This modification led, respectively, to compounds 13 and 14, which are two of the most potent and selective adenosine hA$_3$ receptor antagonists belonging to the new 2-phenylphthalazin-1(2H)-one derivatives reported in this work. Accordingly, we evaluated the effect on hA$_3$ AR affinity of introduction of another methoxy group on the

4-substituent of 14 by synthesizing the 2,4-dimethoxy and 2,5-dimethoxyphenyl-substituted compounds 17 and 18, respectively. The second methoxy substituent introduced at position 5 of the phenyl ring of 14 contributes positively to adenosine hA$_3$ receptor affinity, which showed an 11-fold increase (compare 18 to 14). In fact, the (2,5-dimethoxyphenylureido)-phthalazin-1(2H)-ones 18 is the most potent adenosine hA$_3$ receptor antagonist among this series, with a K_i value of 0.776 nM and at least 10000-fold selectivity over hA$_1$ and hA$_{2A}$ receptors. Unexpectedly, the 2,4-dimethoxy-substituted compound 17 as well as the 4-(4-methylphenyl)- and 4-(2-methylphenyl)-ureido derivatives 15 and 16 did not show any appreciable binding

Table 2. Potencies (IC$_{50}$) at hA$_{2B}$ and hA$_3$ of Some Selected 4-Substituted 2-Phenylphtalazin-1(2H)-one Derivatives

	cAMP assays IC$_{50}$ (nM) or I%	
no.	hA$_{2B}$[a]	hA$_3$[b]
12	0%	28 ± 3
13	57%	18 ± 2
14	16%	17 ± 1.6
18	0%	8.25 ± 0.6
19	34%	1.15 ± 0.02

[a] Percentage of inhibition on cAMP experiments in hA$_{2B}$CHO cells stimulated by 100 nM NECA at different examined compound concentrations (1 nM to 10 μM). [b] IC$_{50}$ values represent the means ± SEMs of three separate experiments in hA$_3$CHO cells, inhibited by 100 nM NECA at different examined compound concentrations (1 nM to 10 μM).

affinity toward the hA$_3$ AR. Introduction of a benzyl-ureido moiety at position 4 of the phthalazin-1(2H)-one scaffold led to compound **19**, which revealed to be 6-fold more active than the homologue **9** at the hA$_3$ receptor (hA$_3$ K_i = 29.6 nM). Finally, the highly profitable methoxy group was introduced at the ortho position on the benzylic group of **19**, yielding compound **20** that unexpectedly showed a 9-fold decreased hA$_3$ affinity.

Among the new PHTZ series, compounds **12−14**, **18**, and **19** possess the highest hA$_3$ affinity and selectivity versus both hA$_1$ and hA$_{2A}$ receptors. To determine also their hA$_3$ versus hA$_{2B}$ selectivity, we tested these derivatives in cAMP assays, which evidenced low or null hA$_{2B}$ affinity, being in general ineffective in inhibiting NECA-stimulated cAMP levels in hA$_{2B}$ CHO cells. Furthermore, the effect of compounds **12−14**, **18**, and **19** in limiting the NECA-inhibited cAMP accumulation in hA$_3$ CHO cells was determined. Coherently with their high hA$_3$ affinity, all of the selected PHTZ derivatives proved to be very potent in this test, showing an antagonistic behavior (Table 2).

Because the new 2-phenylphthalazin-1(2H)-one derivatives reported in this study were conceived as simplified derivatives of the previously synthesized 1,2,4-triazolo[4,3-a]quinoxaline-1-one compounds (TQX series),[18,20,21,24,25] molecular docking studies were performed on all of the PHTZ derivatives (compounds **1−20**) and on the TQX derivative **A**,[18] taken as reference. Moreover, docking simulations were also performed on compound **B**, a quinazoline-4-carboxamide derivative (QZ series) previously reported.[28]

Therefore, all of the selected compounds were docked into the TM binding site of the hA$_3$ AR three-dimensional model, to identify their hypothetical binding modes at this receptor and to analyze possible analogies among the different series. In addition, docking simulations at the hA$_{2A}$ AR were carried out to explain the hA$_3$ versus hA$_{2A}$ selectivity profile of all of these derivatives.

Analysis of the docking results reveals that all of the studied compounds (**1−20**, **A**, and **B**) share a binding pose that is somehow similar in the TM region of the hA$_3$ AR. In fact, at this receptor, ligand recognition occurs in the upper region of the TM bundle, and the tricyclic or bicyclic scaffold of the ligands is surrounded by TMs 3, 5, 6, and 7. Figure 2A shows the hypothetical binding mode of the reference TQX derivative **A** (hA$_3$ AR K_i = 276 nM). This compound is anchored, inside the binding cleft, by three stabilizing hydrogen-bonding interactions with the side chain of Asn250 (6.55). These three hydrogen bonds involve the N^5 atom of the TQX nucleus and the two NH
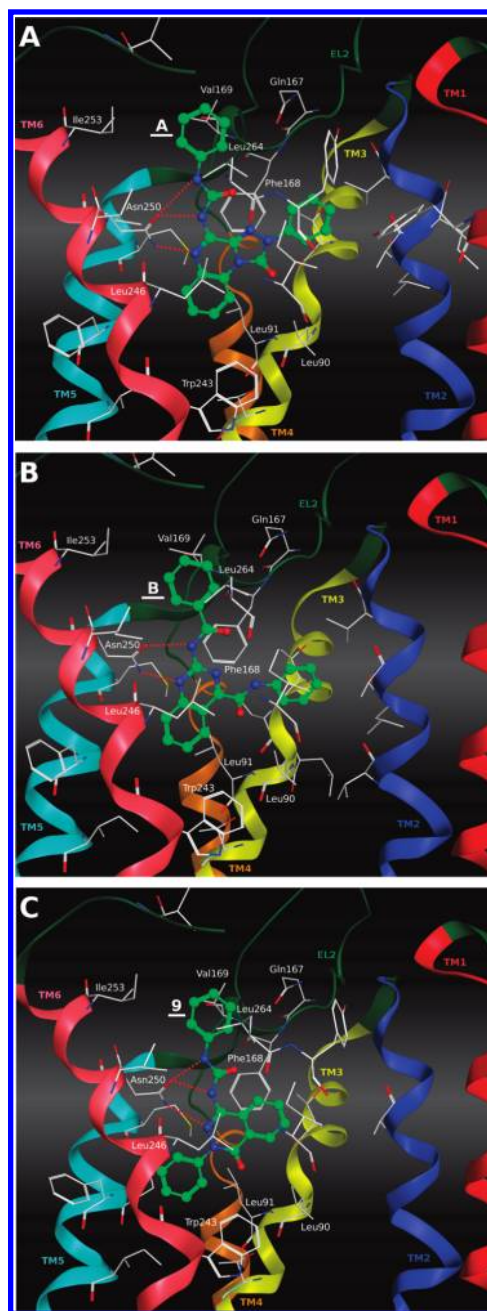

Figure 2. Hypothetical binding modes obtained after docking simulations inside the hA$_3$ AR binding site of (A) compound **A**, (B) compound **B**, and (C) compound **9**. Poses are viewed from the membrane side facing TM6, TM7, and TM1. The view of TM7 is voluntarily omitted. Side chains of some amino acids important for ligand recognition and H-bonding interactions are highlighted. Hydrogen atoms are not displayed.

groups of the 4-ureidic moiety, respectively. The asparagine residue 6.55, conserved among all of the AR subtypes, was already found, through mutagenesis studies,[36,37] to be important for ligand binding at both the hA$_3$ and the hA$_{2A}$ ARs. Compound **A** also forms hydrophobic interactions with many residues of the binding cleft including Ala69 (2.61), Val72 (2.64), Leu90 (3.32), Leu91 (3.33), Phe168 (EL2), Val169 (EL2), Met177 (5.38), Trp243 (6.48), Leu246 (6.51), Ile249 (6.54), Ile253 (6.58), Val259 (EL3), Leu264 (7.35), Tyr265 (7.36), and Ile268 (7.39).

In particular, the planar tricyclic core of the ligand strongly interacts with Phe168 (EL2) and with the highly conserved Trp243 (6.48), an important residue for either receptor activation or for antagonist binding.[37]

As shown in Figure 2B, the hypothetical binding pose of the QZ derivative **B** (hA$_3$ AR K_i = 182 nM), obtained after molecular docking into the three-dimensional model of the hA$_3$ receptor, is very similar to that of compound **A** (Figure 2A). In fact, ligand recognition occurs in the same region of the TM bundle. In particular, the appended phenyl ring on the 4-carboxyamide moiety of **B** is oriented toward TM2, such as the 2-phenyl ring of the TQX derivative **A**, and the 2-benzoylamino group of **B** points toward the extracellular loop region, such as the 4-phenylureido moiety of compound **A**. Moreover, compound **B** forms two H-bonds with Asn250 (6.55) and a strong hydrophobic interaction with Phe168 (EL2).

It is worth noting that in compound **B** the formation of an intramolecular H-bond between the nitrogen at the 3-position of the quinazoline system and the NH of the amide moiety at the 4-position leads to the stabilization of a conformer, which simulates a planar tricycle with similar steric properties to the original TQX analogue (compound **A**). The planarity of the QZ derivative, due to this intramolecular H-bond, seems to increase complementarity with the hA$_3$ receptor; the key role of this intramolecular H-bond was already analyzed in previous docking studies of the QZ derivatives carried out on the rhodopsin-based homology model of hA$_3$ AR.[28]

The hypothetical binding mode, at the hA$_3$ AR, of one of the herein reported 2-phenyl-phthalazin-1(2H)-ones (compound **9**, hA$_3$ AR K_i = 178.4 nM) is displayed in Figure 2C. Molecular docking simulations show that the new compound **9** is efficiently accommodated into the TM binding cavity with the 4-phenylureido substituent directed toward the extracellular loop region. Interestingly, compound **9** maintains all of the crucial interactions already seen for the TQX and QZ derivatives and also a similar binding pose. This ligand forms three hydrogen-bonding interactions with the Asn250 (6.55) side chain, involving the N^3 atom of the PHTZ nucleus and the two NH groups of the ureidic moiety, respectively. In addition, the phthalazinone scaffold forms a $\pi-\pi$ stacking interaction with Phe168 (EL2). Other hydrophobic interactions are established with several residues of the binding cavity, such as Ala69 (2.61), Leu90 (3.32), Leu91 (3.33), Val169 (EL2), Met177 (5.38), Phe182 (5.43), Ile186 (5.47), Trp243 (6.48), Leu246 (6.51), Ile249 (6.54), Ile253 (6.58), Val259 (EL3), Leu264 (7.35), and Ile268 (7.39). The described docking pose of compound **9** reflects more or less the hypothetical binding mode of all of the analyzed 2-phenyl-phthalazin-1(2H)-one derivatives (compounds **1−20**).

Then, electrostatic and hydrophobic interaction contributions between compounds **9**, **A**, and **B** and each amino acid involved in ligand recognition (Figures 3 and 4, respectively) were calculated from the hypothetical binding modes inside the hA$_3$ AR displayed in Figure 2. Analysis of these data confirms the hypothesis of an analogous binding mode at the hA$_3$ AR for the TQX, QZ, and PHTZ derivatives selected in this study.
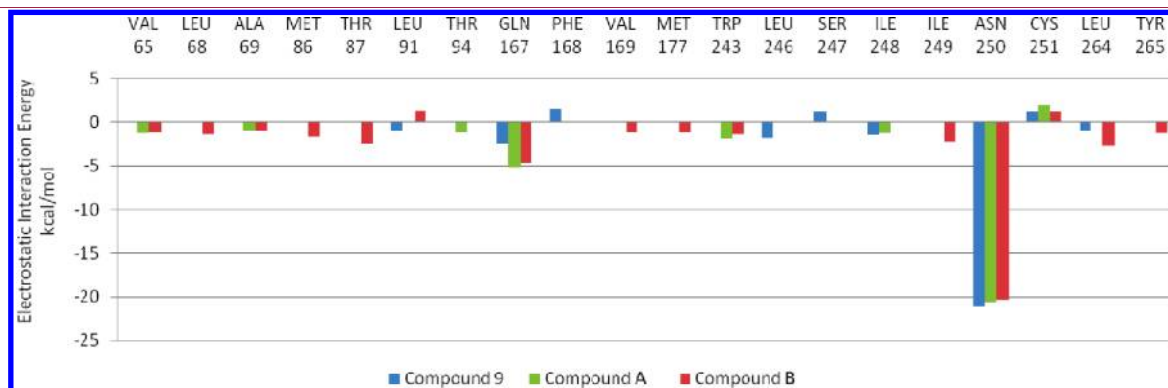

Figure 3. Electrostatic interaction energy (in kcal/mol) between compounds **9**, **A**, and **B** and each single amino acid involved in ligand recognition calculated from the hypothetical binding modes inside the hA$_3$ AR (Figure 2).
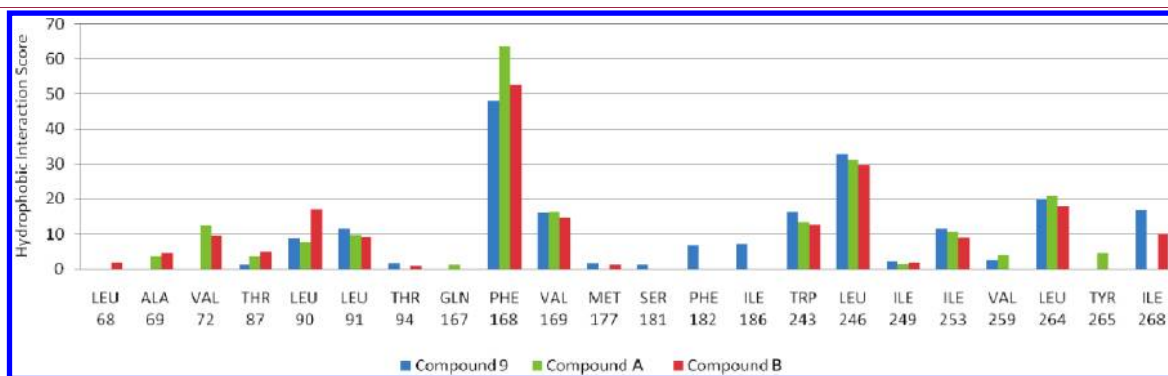

Figure 4. Hydrophobic interaction score (in arbitrary hydrophobic unit) between compounds **9**, **A**, and **B** and each amino acid involved in ligand recognition calculated from the hypothetical binding modes inside the hA$_3$ AR (Figure 2).

As shown in Figure 3, it is clear that, from the electrostatic point of view, one of the most critical residues affecting the affinity at the hA$_3$ AR seems to be the Asn250 (6.55) that is responsible for the stabilizing H-bonding interactions with all of the three ligands. This is supported by the Asn250 electrostatic contribution of around −20 kcal/mol to the whole interaction energy of the three ligand−receptor complexes. Moreover, no significant detrimental electrostatic contributions (positive electrostatic interaction energy) are observed for these complexes.

The hydrophobic interactions mapped in Figure 4 show a similar pattern for all of the three ligand−receptor complexes. In particular, the most important hydrophobic contribution is mediated by Phe168 (EL2), conserved among all ARs, which strongly interacts with the bicyclic/tricyclic core of the ligands. In addition, the ligand scaffold is involved in hydrophobic contacts with Leu90 (3.32), Leu91 (3.33), Trp243 (6.48), Leu246 (6.51), and Ile268 (7.39), while the phenyl ring appended on the ureido/amido moiety interacts with Val169 (EL2), Ile253 (6.58), and Leu264 (7.35).

Some aspects of the SAR of this phthalazine series are very difficult to rationalize. Surprisingly, some substituents, such as phenylamido and benzylamido, that positively affect the affinity in other series of hA$_3$ AR antagonists, showed, in contrast, discouraging results in these new compounds. The herein proposed binding mode seems to partially explain why compounds bearing a 4-ureido substituent possess higher affinity at the hA$_3$ AR than the 4-amido analogues. In fact, the increased affinities of the 4-ureido-derivatives could be due to the formation of an additional H-bonding interaction with the Asn250 (6.55) carbonyl group.

With regard to the substituents on the phenyl ring appended on the 4-ureido moiety, the binding data show that both of their features, electron-donating or electron-withdrawing, and their position play a crucial role in modulating the affinity at the hA$_3$ AR. Considering the herein proposed binding mode at this receptor subtype, it is clear that such substituents are located near the extracellular loop region and can possibly interact with residues belonging to EL2 and EL3 (see the Supporting Information, Figure 1A, for the binding modes of compounds **11**, **14**,

and **16** at the hA$_3$ AR). Because of the difficult characterization and the high plasticity of the loop region, it is hard to accurately predict particular interactions with this part of the ligand and therefore to explain the observed effects of these substituents. Some amino acids possibly involved in interactions with the substituted phenyl ring are Gln167 (EL2), Val169 (EL2), Met174 (5.35), Ile253 (6.58), Val259 (EL3), and Leu264 (7.35). Calculation of the per residue electrostatic and hydrophobic contributions to the interaction energy was performed on the docking poses of compounds **11**, **14**, and **16** at the hA$_3$ AR to analyze possible differences. However, as expected, no significant differences were seen considering these ligand−receptor complexes (see the Supporting Information, Figure 1B,C), and so, no clues about the role of these different substituents were obtained. Further studies are in progress in our laboratory to better define the extracellular loops conformation that could be responsible for the interaction with the substituents at the 4-position of these ligands.

As far as the hA$_{2A}$ AR is concerned, docking simulations performed for compounds **1**−**20** revealed no good binding poses at this receptor subtype, as highlighted by the docking pose of compound **9** at the hA$_{2A}$ AR displayed in Figure 5A. In fact, at the hA$_{2A}$ AR, compound **9** resulted to be turned of 180° as compared to the docking pose of the same compound inside the hA$_3$ AR binding site, probably due to the presence of a Glu169 and of the steric hindrance of the substituent at the 4-position. As a consequence of this flipped orientation, compound **9** was not able to strongly interact with the critical residues Asn253 (6.55) or Glu169 (EL2) through H-bonds as instead previously noticed for the crystallographic binding pose of ZM241385 at the hA$_{2A}$ AR[33] and found in all other docked compounds possessing antagonist activity at the hA$_{2A}$ AR.[38] Indeed, analyzing the per residue electrostatic and hydrophobic contributions for the docking pose of compound **9** inside the hA$_{2A}$ AR (Figure 5B, C, respectively), it is evident the lack of any strong electrostatic interaction with residues of the binding site and the presence of only few strong hydrophobic interactions, such as the one with Phe168. This finding can explain the low or null affinity at the A$_{2A}$
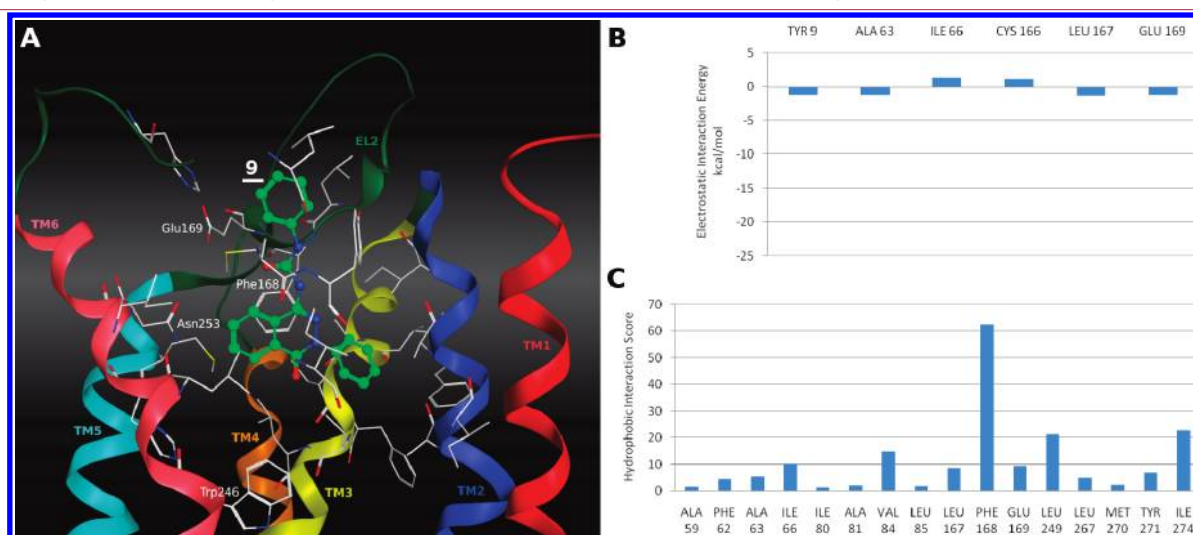

Figure 5. (A) Hypothetical binding mode obtained after docking simulation inside the hA$_{2A}$ AR binding site of compound **9**. The pose is viewed from the membrane side facing TM1, TM6, and TM7. The view of TM7 is voluntarily omitted. Hydrogen atoms are not displayed. (B) Electrostatic interaction energy (in kcal/mol) between compound **9** and each single amino acid involved in ligand recognition calculated from the hypothetical binding mode inside the hA$_{2A}$ AR. (C) Hydrophobic interaction score (in arbitrary hydrophobic unit) between compound **9** and each amino acid involved in ligand recognition calculated from the hypothetical binding mode inside the hA$_{2A}$ AR.

AR subtype of all of the compounds (1−20) reported in this work.

In conclusion, molecular docking studies of the newly synthesized 2-phenylphthalazin-1(2H)-ones, performed at the hA3 AR, revealed for these compounds a binding mode similar to that of the previously reported TQX and QZ derivatives, as was expected from the simplification approach. These three classes of hA3 AR antagonists show analogous interactions with the binding cavity of the receptor as confirmed by the analysis of the electrostatic and hydrophobic contributions to the interaction energy. Further studies are in progress in our laboratories to better clarify the structural requirements for profitable hA3 receptor−ligand interaction of this class of compounds and to develop new PHTZ derivatives with higher hA3 AR affinity.

■ EXPERIMENTAL SECTION

Chemistry. Silica gel plates (Merck F_{254}) and silica gel 60 (Merck; 70−230 mesh) were used for analytical and column chromatography, respectively. All melting points were determined on a Gallenkamp melting point apparatus. Microanalyses were performed with a Perkin-Elmer 260 elemental analyzer for C, H, and N, and the results were within ±0.4% of the theoretical values except where stated otherwise. The IR spectra were recorded with a Perkin-Elmer Spectrum RX I spectrometer in Nujol mulls and are expressed in cm^{-1}. The ^{1}H NMR spectra were obtained with a Bruker Avance 400 MHz instrument. The chemical shifts are reported in δ (ppm) and are relative to the central peak of the solvent, which was always DMSO-d_6. All of the exchangeable protons were confirmed by addition of D_2O. Used are the following abbreviations: s, singlet; d, doublet; dd, double doublet; t, triplet; m, multiplet; br, broad; and ar, aromatic protons.

Synthesis of 4-Hydroxy-2-phenylphthalazin-1(2H)-one 21[30]. A mixture of phenylhydrazine (81.0 mmol) and phthalic anhydride (67.5 mmol) in 10% HCl (100 mL) was heated at reflux for 9 h. After it was cooled, the resulting solid was collected by filtration, washed with water, and recrystallized. Yield, 75%; mp 212−213 °C (EtOH) (p.f. lit.[31] 213.85 °C). ^{1}H NMR: 7.37 (t, 1H, ar, J = 7.13 Hz), 7.50 (t, 2H, ar, J = 7.50 Hz), 7.64 (d, 2H, ar, J = 7.76 Hz), 7.92−8.04 (m, 3H, ar), 8.31 (d,1H, ar, J = 7.44 Hz), 11.85 (br s, 1H, NH). IR: 1642, 3400−2000. Anal. ($C_{14}H_{10}N_2O_2$) C, H, N.

Synthesis of 4-Chloro-2-phenylphthalazin-1(2H)-one 22. A mixture of compound 21[30] (25.0 mmol) in a large excess of $POCl_3$ (6 mL) was heated at reflux for 4 h. After it was cooled (0 °C), the resulting solution was slowly quenched with cold NaOH solution (5M, 100 mL) yielding a suspension that was stirred at room temperature for 2 h. The resulting brown solid was collected by filtration and washed with water. Yield, 65%; mp 130−131 °C (EtOH) (p.f. lit.[32] 130 °C EtOH/H_2O). ^{1}H NMR: 7.45 (t, 1H, ar, J = 7.13 Hz), 7.54 (t, 2H, ar, J = 7.75 Hz), 7.62 (d, 2H, ar, J = 7.72 Hz), 8.02−8.13 (m, 3H, ar), 8.38 (d, 1H, ar, J = 7.77 Hz). IR: 1675. Anal. ($C_{14}H_9ClN_2O$) C, H, N.

Synthesis of 4-Hydrazino-2-phenylphthalazin-1(2H)-one 23. A mixture of the 4-chloro derivative 22[32] (5.65 mmol), hydrazine sulfate salt (11.3 mmol), and an excess of anhydrous hydrazine (100%, 2.9 mL) in ethylene glycol (20 mL) was heated at 115 °C for 1 h. After it was cooled, the reaction mixture was diluted with water (30 mL), and the resulting solid was collected by filtration. Yield, 63%; mp 190−191 °C (ethylene glycol/H_2O) (p.f. lit.[32] 190 °C). ^{1}H NMR: 4.13 (s, 2H, NH_2), 7.33 (t, 1H, ar, J = 7.28 Hz), 7.47 (t, 2H, ar, J = 7.68 Hz), 7.81 (d, 2H, ar, J = 7.76 Hz), 7.85−7.95 (m, 2H, ar), 8.13 (d, 1H, ar, J = 7.76 Hz), 8.20 (s, 1H, NH), 8.33 (d, 1H, ar, J = 7.52 Hz). IR: 1642, 3354. Anal. ($C_{14}H_{12}N_4O$) C, H, N.

Synthesis of 4-Amino-2-phenylphthalazin-1(2H)-one 1. Raney nickel (2400, slurry, in H_2O, 24 g) was added to a solution of the hydrazino derivative 23 (5.0 mmol) in ethanol (200 mL). The reaction mixture was hydrogenated in a Parr apparatus at 15 psi for 12 h. After elimination of the catalyst by filtration, the ethanol solution was evaporated under reduced pressure. The resulting solid was worked up with a little ethyl ether and collected by filtration. Yield, 81%; mp 188−200 °C (EtOAc). ^{1}H NMR: 6.31 (s, 2H, NH_2), 7.34 (t, 1H, ar, J = 7.18 Hz), 7.47 (t, 2H, ar, J = 7.75 Hz), 7.64 (d, 2H, ar, J = 7.52 Hz), 7.88 (t, 1H, ar, J = 7.18 Hz), 7.95 (t, 1H, ar, J = 7.54 Hz), 8.15 (d, 1H, ar, J = 7.68 Hz), 8.33 (d, 1H, ar, J = 7.68 Hz). IR: 1625, 3214, 3318, 3422. Anal. ($C_{14}H_{11}N_3O$) C, H, N.

Synthesis of 4-Acetylamino-2-phenylphthalazin-1(2H)-one 2 and 4-Diacetylamino-2-phenylphthalazin-1(2H)-one 3. A solution of acetyl chloride (1.85 mmol) in anhydrous tetrahydrofuran (5 mL) was dropwise added (30 min) to a cooled (5 °C) solution of the 4-amino derivative 1 (1.68 mmol) in anhydrous tetrahydrofuran (10 mL) and anhydrous pyridine (3.3 mmol). The reaction mixture was stirred at room temperature for 24 h and then diluted with EtOAc (70 mL). The resulting solution was washed with water (50 mL × 3), then with $NaHCO_3$ solution (2.5%, 30 mL), and finally again with water (50 mL). Evaporation under reduced pressure of the dried (Na_2SO_4) ethyl acetate solution yielded a solid (mixture 3:1 of compounds 2 and 3, ^{1}HNMR analysis) which was worked up with the minimal amount of diethyl ether and collected by filtration. Separation of compounds 2 and 3 was performed by using silica gel column cromatography, eluting system CH_2Cl_2/MeOH 9:1. Evaporation of the first eluates afforded compound 3, while the central eluates contained the monoacetyl derivative 2.

Compound 2. Yield, 49%; mp 197−199 °C (2-methoxyethanol). ^{1}H NMR: 2.16 (s, 3H, CH_3), 7.43 (t, 1H, ar, J = 6.96 Hz), 7.53 (t, 2H, ar, J = 7.74 Hz), 7.62 (d, 2H, ar, J = 7.96 Hz), 7.86 (d, 1H, ar, J = 7.76 Hz), 7.92−8.01 (m, 2H, ar), 8.35 (d, 1H, ar, J = 7.68 Hz), 10.35 (s, 1H, NH). IR: 1672, 3248. Anal. ($C_{16}H_{13}N_3O_2$) C, H, N.

Compound 3. Yield, 15%; mp 185−186 °C (2-methoxyethanol). ^{1}H NMR: 2.38 (s, 6H, 2CH_3), 7.45 (t, 1H, ar, J = 7.36 Hz), 7.54 (t, 2H, ar, J = 7.72 Hz), 7.63 (d, 2H, ar, J = 7.72 Hz), 7.92 (d, 1H, ar, J = 7.12 Hz), 7.98 (m, 2H, ar), 8.42 (d, 1H, ar, J = 7.12 Hz). IR: 1673, 1697, 1729. Anal. ($C_{18}H_{15}N_3O_3$) C, H, N.

General Procedure for the Synthesis of 4-Aroylamino-2-phenylphthalazin-1(2H)-ones 4−7 and 4-Phenylacetylamino-2-phenylphthalazin-1(2H)-one 8. A solution of the suitable aroyl chloride (compounds 4−7) or phenylacetyl chloride (8) (6.0 mmol) in anhydrous tetrahydrofuran (5 mL) was dropwise added (30 min) to a cooled (5 °C) solution of the 4-amino derivative 1 (2.0 mmol) in anhydrous tetrahydrofuran (20 mL) and anhydrous pyridine (20 mmol). The reaction mixture was stirred at room temperature until the disappearance of the starting derivative 1 (TLC monitoring, 15−72 h). The resulting suspension (compounds 5−8) was diluted with water (50 mL) and extracted with EtOAc (70 mL). The organic layer was washed with water (50 mL × 2), then with $NaHCO_3$ solution (2.5%, 50 mL), and finally again with water (50 mL). Evaporation under reduced pressure of the dried (Na_2SO_4) ethyl acetate solution yielded a solid, which was worked up with the minimal amount of diethyl ether and collected by filtration. Compounds 6−8 were recrystallized, while compound 5 was purified by silica gel column chromatography, eluting system CH_2Cl_2/EtOAc 8:2, and then recrystallized. For derivative 4, the reaction mixture was filtered, and the solid was washed with water and recrystallized.

Compound 4. Yield, 39%; mp 201−202 °C (EtOH). ^{1}H NMR: 7.44 (t, 1H, ar, J = 7.34 Hz), 7.52−7.60 (m, 4H, ar), 7.63−7.68 (m, 3H, ar), 7.85 (d, 1H, ar, J = 8.64 Hz) 7.95−8.02 (m, 2H, ar), 8.07 (d, 2H, ar, J = 7.40 Hz), 8.39 (d, 1H, ar, J = 7.12 Hz), 10.91 (s, 1H, NH). IR: 1651, 1670. Anal. ($C_{21}H_{15}N_3O_2$) C, H, N.

Compound 5. Yield, 27%; mp 190−191 °C (2-methoxyethanol). ^{1}H NMR: 7.44 (t, 1H, ar, J = 6.96 Hz), 7.54 (t, 2H, ar, J = 8.62 Hz), 7.63−7.68 (m, 4H, ar), 7.85 (d, 1H, ar, J = 7.44 Hz) 7.94−7.98 (m, 2H, ar), 8.08 (d, 2H, ar, J = 8.56 Hz), 8.39 (d, 1H, ar, J = 7.44 Hz), 11.00 (s, 1H, NH). IR: 1671, 3072. Anal. ($C_{21}H_{14}ClN_3O_2$) C, H, N.

Compound 6. Yield, 55%; mp 203−204 °C (EtOH). ^{1}H NMR: 3.87 (s, 3H, OCH$_3$), 7.10 (d, 2H, ar, J = 8.88 Hz), 7.44 (t, 1H, ar, J = 7.34 Hz), 7.54 (t, 2H, ar, J = 7.74 Hz), 7.64 (d, 2H, ar, J = 8.12 Hz), 7.80 (d, 1H, ar, J = 8.88 Hz) 7.94−8.01 (m, 2H, ar), 8.05 (d, 2H, ar, J = 8.88 Hz), 8.39 (d, 1H, ar, J = 8.88 Hz), 10.74 (s, 1H, NH). IR: 1670, 3068. Anal. (C$_{22}$H$_{17}$N$_3$O$_3$) C, H, N.

Compound 7. Yield, 71%; mp 193−194 °C (MeOH). ^{1}H NMR: 6.75 (d, 1H, ar, J = 3.36 Hz), 7.42−7.45 (m, 2H, ar), 7.54 (t, 2H, ar, J = 7.66 Hz), 7.64 (d, 2H, ar, J = 8.32 Hz), 7.83 (d, 1H, ar, J = 7.72 Hz), 7.95−8.01 (m, 3H, ar), 8.39 (d, 1H, ar, J = 7.28 Hz), 10.83 (s, 1H, NH). IR: 1659. Anal. (C$_{19}$H$_{13}$N$_3$O$_3$) C, H, N.

Compound 8. Yield, 40%; mp 194−195 °C (MeOH). ^{1}H NMR: 3.80 (s, 2H, CH$_2$), 7.26−7.29 (m, 1H, ar), 7.33−7.45 (m, 5H, ar), 7.53 (t, 2H, ar, J = 7.66 Hz), 7.61 (d, 2H, ar, J = 7.64 Hz), 7.72 (d, 1H, ar, J = 7.44 Hz), 7.91−7.97 (m, 2H, ar), 8.34 (d, 1H, ar, J = 7.44 Hz), 10.58 (s, 1H, NH). IR: 1650, 1666, 3242. Anal. (C$_{22}$H$_{17}$N$_3$O$_2$) C, H, N.

General Procedure for the Synthesis of 4-Arylureido-2-phenylphthalazin-1(2H)-ones 9−13, 15, and 16 and 4-Aralkylureido-2-phenylphthalazin-1(2H)-ones 19 and 20. A mixture of **1** (1.3 mmol) and an equimolar amount of the suitable aryl or aralkyl isocyanate in anhydrous methylene chloride (10 mL) was stirred under nitrogen atmosphere for 2−15 days. For compounds **9, 10, 12, 13,** and **19,** the reaction mixture was kept at room temperature, while derivatives **11, 15, 16,** and **20** were obtained by heating at 50 °C. Further additions of the starting isocyanate (0.5−1 equivalent) were performed when compound **1** was still present in the mixture (TLC monitoring) after 48 h from the beginning of the reaction. The resulting suspension was filtered, and the solid phase was resuspended in a mixture of cyclohexane/EtOAc 3:7 (80 mL) and kept under stirring for 4 h. The crude product was collected by filtration, washed many times with cyclohexane/EtOAc 3:7, and recrystallized from 2-methoxyethanol. It was not possible to recrystallize compound **10** since it resulted unstable upon heating in the suitable crystallization solvent, that is, DMF. Compound **10** was purified by repeated washing with hot ethanol. TLC analysis (cyclohexane/EtOAc 3:7), ^{1}H NMR spectrum, and melting point of crude **10** showed that it was pure enough to be tested in the binding assays.

Compound 9. Yield, 40%; mp >300 °C. ^{1}H NMR: 7.00 (t, 1H, ar, J = 7.20 Hz), 7.29 (t, 2H, ar, J = 7.08 Hz), 7.43−7.47 (m, 3H, ar), 7.54 (t, 2H, ar, J = 7.22 Hz) 7.70 (d, 2H, ar, J = 7.48 Hz), 7.96−8.02 (m, 2H, ar), 8.16 (d, 1H, ar, J = 7.56 Hz); 8.38 (d, 1H, ar, J = 7.52 Hz), 9.55 (br s, 1H, NH), 9.83 (br s, 1H, NH). IR: 1672, 1697, 3360, 3420, 3495, 3522, 3564. Anal. (C$_{21}$H$_{16}$N$_4$O$_2$) C, H, N.

Compound 10. Yield, 76%; mp 262−264 °C (crude). ^{1}H NMR: 7.35 (d, 2H, ar, J = 8.72 Hz), 7.42 (t, 1H, ar, J = 7.34 Hz), 7.49−7.55 (m, 4H, ar), 7.69 (d, 2H, ar, J = 7.48 Hz), 7.95−8.04 (m, 2H, ar), 8.12 (d, 1H, ar, J = 7.91 Hz); 8.40 (d, 1H, ar, J = 7.68 Hz), 9.34 (s, 1H, NH), 9.63 (s, 1H, NH). IR: 1677, 1698, 3067, 3272. Anal. (C$_{21}$H$_{15}$ClN$_4$O$_2$) C, H, N.

Compound 11. Yield, 49%; mp 251−252 °C. ^{1}H NMR: 7.04 (t, 1H, ar, J = 8.34 Hz), 7.30 (t, 1H, ar, J = 7.78 Hz), 7.38 (d, 1H, ar, J = 7.96 Hz), 7.44−7.57 (m, 1H, ar), 7.54 (t, 2H, ar, J = 7.60 Hz), 7.62 (d, 2H, ar, J = 7.48 Hz), 7.97−8.06 (m, 2H, ar), 8.22 (d, 1H, ar, J = 8.28 Hz), 8.34−8.40 (m, 2H, ar), 9.87 (s, 1H, NH), 9.91 (s, 1H, NH). IR: 1663, 1680, 3152, 3277. Anal. (C$_{21}$H$_{15}$ClN$_4$O$_2$) C, H, N.

Compound 12. Yield, 45%; mp 259−260 °C. ^{1}H NMR: 3.72 (s, 3H, OCH$_3$), 6.88 (d, 2H, ar, J = 7.52 Hz), 7.35 (d, 2H, ar, J = 7.56 Hz), 7.43 (t, 1H, ar, J = 7.34 Hz), 7.54 (t, 2H, ar, J = 7.16 Hz), 7.70 (d, 2H, ar, J = 7.92 Hz), 7.94−8.04 (m, 2H, ar), 8.19 (d, 1H, ar, J = 7.96 Hz), 8.39 (d, 1H, ar, J = 7.76 Hz), 9.25 (s, 1H, NH), 9.50 (s, 1H, NH). IR: 1655, 1682, 3097, 3143, 3193, 3270. Anal. (C$_{22}$H$_{18}$N$_4$O$_3$) C, H, N.

Compound 13. Yield, 64%; mp 244−246 °C. ^{1}H NMR: 3.34 (s, 3H, OCH$_3$), 6.59 (d, 1H, ar, J = 8.24 Hz), 6.99 (d, 1H, ar, J = 8.12 Hz), 7.11 (s, 1H, ar), 7.19 (t, 1H, ar, J = 8.14 Hz), 7.43 (t, 1H, ar, J = 7.38 Hz), 7.54 (t, 2H, ar, J = 7.64 Hz), 7.71 (d, 2H, ar, J = 8.32 Hz), 7.95−8.04 (m, 2H, ar), 8.17 (d, 1H, ar, J = 7.88 Hz), 8.39 (d, 1H, ar, J = 7.84 Hz), 9.29 (s, 1H, NH), 9.63 (s, 1H, NH). IR: 1668, 1694, 3098, 3143, 3201, 3270. Anal. (C$_{22}$H$_{18}$N$_4$O$_3$) C, H, N.

Compound 15. Yield, 46%; mp 261−263 °C. ^{1}H NMR: 2.25 (s, 3H, CH$_3$), 7.10 (d, 2H, ar, J = 8.20 Hz), 7.33 (d, 2H, ar, J = 8.36 Hz), 7.43 (t, 1H, ar, J = 7.38 Hz), 7.54 (t, 2H, ar, J = 7.72 Hz), 7.70 (d, 2H, ar, J = 8.12 Hz), 7.94−8.04 (m, 2H, ar), 8.18 (d, 1H, ar, J = 7.88 Hz), 8.39 (d, 1H, ar, J = 7.84 Hz), 9.26 (s, 1H, NH), 9.54 (s, 1H, NH). IR: 1667, 1688, 3191. Anal. (C$_{22}$H$_{18}$N$_4$O$_2$) C, H, N.

Compound 16. Yield, 51%; mp 247−249 °C. ^{1}H NMR: 1.86 (s, 3H, CH$_3$), 6.96 (t, 1H, ar, J = 7.36 Hz), 7.11−7.17 (m, 2H, ar), 7.45 (t, 1H, ar, J = 7.32 Hz), 7.54 (t, 2H, ar, J = 7.68 Hz), 7.65 (d, 2H, ar, J = 7.76 Hz), 7.87 (d, 1H, ar, J = 7.96 Hz), 7.96−8.06 (m, 2H, ar), 8.34 (d, 1H, ar, J = 7.92 Hz), 8.39 (d, 1H, ar, J = 7.24 Hz), 9.39 (s, 1H, NH), 9.60 (s, 1H, NH). IR: 1659, 1681, 3136, 3190. Anal. (C$_{22}$H$_{18}$N$_4$O$_2$) C, H, N.

Compound 19. Yield, 41%; mp 218−219 °C. ^{1}H NMR: 4.36 (d, 2H, CH$_2$, J = 5.68 Hz), 7.24−7.33 (m, 5H, ar), 7.37−7.40 (m, 1H, ar); 7.45 (t, 2H, ar, J = 7.54 Hz), 7.59 (d, 2H, ar, J = 7.64 Hz), 7.85 (t, 1H, NH, J = 5.54 Hz), 7.92−8.02 (m, 2H, ar), 8.20 (d, 1H, ar, J = 7.76 Hz), 8.36 (d, 1H, ar, J = 7.20 Hz), 9.23 (s, 1H, NH). IR: 1678, 3140, 3258. Anal. (C$_{22}$H$_{18}$N$_4$O$_2$) C, H, N.

Compound 20. Yield, 48%; mp 244−246 °C. ^{1}H NMR: 3.66 (s, 3H, OCH$_3$), 4.31 (d, 2H, CH$_2$, J = 5.28 Hz), 6.86 (t, 1H, ar, J = 7.44 Hz), 6.96 (d, 1H, ar, J = 8.24 Hz), 7.17−7.27 (m, 2H, ar), 7.38−7.42 (m, 1H, ar), 7.47 (t, 2H, ar, J = 7.66 Hz), 7.60 (d, 2H, ar, J = 7.68 Hz), 7.83 (br s, 1H, NH), 7.92−8.01 (m, 2H, ar), 8.24 (d, 1H, ar, J = 8.04 Hz), 8.36 (d, 1H, ar, J = 7.08 Hz), 9.35 (s, 1H, NH). IR: 1657, 1673, 3314. Anal. (C$_{23}$H$_{20}$N$_4$O$_3$) C, H, N.

Synthesis of 4-(2-Methoxyphenyl)ureido-2-phenylphthalazin-1(2H)-one 14. A mixture of **1** (2.0 mmol) and 2-methoxyphenyl isocyanate (3.0 mmol) in anhydrous THF (twice-distilled, 30 mL) was stirred at 50 °C under nitrogen atmosphere for a total time of 30 h. After 12 h, further isocyanate was portionwise added (0.3 mmol × 6) at 3 h intervals to the reaction mixture. The resulting suspension was filtered, and the solid phase was resuspended in a mixture of cyclohexane/EtOAc 3:7 (80 mL) and kept under stirring for 4 h. The crude product was collected by filtration, washed many times with cyclohexane/EtOAc 3:7, and recrystallized. Yield, 40%; mp 267−268 °C (2-methoxyethanol). ^{1}H NMR: 3.34 (s, 3H, OCH$_3$), 6.88−7.00 (m, 3H, ar), 7.45 (t, 1H, ar, J = 7.13 Hz), 7.56 (t, 2H, ar, J = 7.38 Hz), 7.69 (d, 2H, ar, J = 7.84 Hz), 7.96−8.05 (m, 2H, ar), 8.15 (d, 1H, ar, J = 7.80 Hz), 8.35−8.40 (m, 2H, ar), 9.71 (s, 1H, NH), 9.90 (s, 1H, NH). IR 1655, 1681, 3186. Anal. (C$_{22}$H$_{18}$N$_4$O$_3$) C, H, N.

General Procedure for the Synthesis of 4-(2,4-Dimethoxyphenylureido)- and 4-(2,5-Dimethoxyphenylureido)-2-phenylphthalazin-1(2H)-ones 17 and 18. A mixture of **1** (0.63 mmol) and an equimolar amount of the suitable dimethoxyphenyl isocyanate in anhydrous methylene chloride (7.0 mL) was stirred under nitrogen atmosphere for 1 day. Then, the suspension was heated at 40−45 °C, and further isocyanate (0.31 mmol × 5) was added at 3 day intervals to the reaction mixture. Heating was maintained for 18 days. The resulting solid was filtered, washed with a small amount of fresh methylene chloride, and then recrystallized from 2-methoxyethanol.

Compound 17. Yield, 42%; mp 257−259 °C. ^{1}H NMR: 3.34 (s, 3H, OCH$_3$), 3.72 (s, 3H, OCH$_3$), 6.48 (dd, 1H, ar, J = 8.84, 2.68 Hz), 6.53 (s, 1H, ar), 7.45 (t, 1H, ar, J = 7.36 Hz), 7.56 (t, 2H, ar, J = 7.76 Hz), 7.68 (d, 2H, ar, J = 8.20 Hz), 7.95−8.05 (m, 3H, ar), 8.36−8.40 (m, 2H, ar), 9.60 (s, 1H, NH), 9.75 (s, 1H, NH). IR: 1660, 3061, 3139, 3186, 3266. Anal. (C$_{23}$H$_{20}$N$_4$O$_4$) C, H, N.

Compound 18. Yield, 34%; mp 294−296 °C. ^{1}H NMR: 3.32 (s, 3H, OCH$_3$), 3.68 (s, 3H, OCH$_3$), 6.53 (dd, 1H, ar, J = 8.92, 3.04 Hz), 6.84 (d, 1H, ar, J = 8.92 Hz), 7.45 (t, 1H, ar, J = 7.36 Hz), 7.55 (t, 2H, ar, J = 7.76 Hz), 7.68 (d, 2H, ar, J = 8.12 Hz), 7.85 (s, 1H, ar), 7.95−8.05 (m, 2H, ar), 8.32 (d, 1H, ar, J = 7.80 Hz), 8.39 (d, 1H, ar, J = 7.88 Hz),

9.72 (s, 1H, NH), 9.79 (s, 1H, NH). IR: 1657, 1681, 3285. Anal. ($C_{23}H_{20}N_4O_4$) C, H, N.

Molecular Modeling. All modeling studies were carried out on a 20 CPU (Intel Core2 Quad CPU 2.40 GHz) Linux cluster. Homology modeling, energy calculation, and analyses of docking poses were performed using the Molecular Operating Environment (MOE, version 2009.10) suite.[39] The software package MOPAC (version 7),[40] implemented in MOE suite, was utilized for all quantum mechanical calculations. Docking simulations were performed using GOLD suite (version 1.3.2).[41]

Homology Model of the hA$_3$ AR. On the basis of the assumption that GPCRs share similar TM boundaries and overall topology, a homology model of the hA$_3$ AR was constructed, as previously reported,[29,34] using as template the recently published crystal structure of hA$_{2A}$ receptor (PDB code: 3EML).[33] The amino acid sequences of TM helices of the hA$_3$ receptor were aligned with those of the template, and then, the hA$_3$ AR homology model was constructed using the homology modeling protocol implemented in MOE as detailed in the Supporting Information.

The numbering of the amino acids follows the arbitrary scheme by Ballesteros and Weinstein. According to this scheme, each amino acid identifier starts with the helix number, followed by the position relative to a reference residue among the most conserved amino acid in that helix. The number 50 is arbitrarily assigned to the reference residue.[42]

Protein stereochemistry evaluation was then performed by several tools (Ramachandran plot; backbone bond lengths, angles, and dihedral plots; clash contacts report; and rotamers strain energy report) implemented in MOE suite.[39,43]

Molecular Docking of hA$_3$ AR Antagonists. Ligand structures were built using MOE builder tool, part of the MOE suite,[39] and were subjected to MMFF94x energy minimization until the rms conjugate gradient was <0.05 kcal mol^{-1} Å^{-1}. Partial charges for the ligands were calculated using PM3/ESP methodology.

Four different programs were used to calibrate our docking protocols: MOE-Dock,[39] GOLD,[41] Glide,[44] and PLANTS.[45] In particular, 4-(2-[7-amino-2-(2-furyl)[1,2,4]-triazolo[2,3-a][1,3,5]triazin-5-ylamino]ethyl)phenol (ZM-241385) was redocked into the crystal structure of the hA$_{2A}$ AR (PDB code: 3EML) with different docking algorithms and scoring functions, as already described.[29,46] Then, rmsd values between predicted and crystallographic positions of ZM-241385 were calculated for each of the docking algorithms. The results showed that docking simulations performed with GOLD gave the lowest rmsd value, the lowest mean rmsd value, and the highest number of poses with rmsd value <2.5 Å.[29,46]

On the basis of the best docking performance, all antagonist structures were docked into the hypothetical TM binding site of the hA$_3$ AR model and that of the hA$_{2A}$ AR crystal structure by using the docking tool of the GOLD suite.[41] Searching was conducted within a user-specified docking sphere, using the Genetic Algorithm protocol and the GoldScore scoring function. GOLD performed a user-specified number of independent docking runs (25 in our specific case) and wrote the resulting conformations and their scores in a molecular database file. The resulting docked complexes (ligand and side chains of residues at 4.5 Å from the ligand) were subjected to MMFF94x energy minimization until the rms conjugate gradient was <1 kcal mol^{-1} Å^{-1}. Partial charges for the ligands were calculated using MOPAC and in particular using PM3/ESP methodology.

Prediction of antagonist−receptor complex stability (in terms of corresponding pK_i value) and the quantitative analysis for non-bonded intermolecular interactions (H-bonds, transition metal, water bridges, hydrophobic, and electrostatic) was calculated and visualized using several tools implemented in MOE suite.[39] Electrostatic and hydrophobic contributions to the binding energy of individual amino acids have been calculated as implemented in MOE suite.[39] To estimate the electrostatic contributions, atomic charges for the ligands were calculated using PM3/ESP

methodology. Partial charges for protein amino acids were calculated on the basis of the AMBER99 force field.

Pharmacological Assays. *Human Cloned A$_1$, A$_{2A}$, and A$_3$ AR Binding Assay.* Binding experiments at hA$_1$ and hA$_{2A}$ ARs, stably expressed in CHO cells, were performed as previously described,[47] using [^{3}H]DPCPX and [^{3}H]NECA, respectively, as radioligands. Displacement of [^{125}I]AB-MECA from hA$_3$ AR, stably expressed in CHO cells, was performed as reported in ref 20.

Measurement of cAMP Levels on CHO Cells Transfected with Human A$_{2B}$ and A$_3$ ARs. Intracellular cAMP levels were measured using a competitive protein binding method.[48] CHO cells (~60000), stably expressing hA$_{2B}$ or hA$_3$ ARs, were plated in 24-well plates. After 48 h, the medium was removed, and the cells were incubated at 37 °C for 15 min with 0.5 mL di DMEM in the presence of Ro20-1724 [4-(3-butoxy-4-methoxybenzyl)imidazolidin-2-one] (20 μM) and adenosine deaminase (1 U/mL). A stock 1 mM solution of the tested compound was prepared in DMSO, and subsequent dilutions were accomplished in distilled water. The antagonistic profile of the new compound toward hA$_{2B}$ AR was evaluated assessing its ability to inhibit 100 nM NECA-mediated accumulation of cAMP. The antagonistic profile of the new compound toward hA$_3$ AR was evaluated by assessing its ability to counteract 100 nM NECA-mediated inhibition of cAMP accumulation stimulated by 1 μM forskolin. Cells were incubated in the reaction medium (15 min at 37 °C) with different compound concentrations (1 nM to 10 μM) and then treated with NECA. The reaction was terminated by removing the medium and adding 0.4 N HCl. After 30 min, the lysate was neutralized with 4 N KOH, and the suspension was centrifuged at 800g for 5 min. To determine cyclic AMP production, the binding protein, prepared from beef adrenal glands, was incubated with [^{3}H]cAMP (2 nM) in distilled water, 50 μL of cell lysate, or standard cAMP (0−16 pmol) at 4 °C for 150 min in a total volume of 300 μL. Bound radioactivity was separated by rapid filtration through GF/C glass fiber filters and washed twice with 4 mL of 50 mM Tris/HCl, pH 7.4. The radioactivity was measured by liquid scintillation spectrometry.

Data Analysis. The concentration of the tested compounds that produced 50% inhibition of specific [^{3}H]DPCPX, [^{3}H]NECA, and [^{125}I]AB-MECA binding (IC$_{50}$) was calculated using a nonlinear regression method implemented by the InPlot program (Graph-Pad, San Diego, CA) with five concentrations of displacer, each performed in triplicate. Inhibition constants (K_i) were calculated according to the Cheng−Prusoff equation.[49] The K_d values of [^{3}H]DPCPX, [^{3}H]NECA, and [^{125}I]AB-MECA in hA$_1$, hA$_{2A}$, and hA$_3$ ARs in CHO cell membranes were 3, 30, and 1.4 nM, respectively. IC$_{50}$ values obtained in cAMP assays were calculated by nonlinear regression analysis using the equation for a sigmoid concentration−response curve (Graph-Pad).

■ ASSOCIATED CONTENT

ⓢ Supporting Information. Combustion analysis data of the newly synthesized compounds, methodological details about the hA$_3$ AR homology model construction, hypothetical binding modes at the hA$_3$ AR of compounds **11**, **14**, and **16** with their relative per residue electrostatic interaction energies and hydrophobic interaction scores. This material is available free of charge via the Internet at http://pubs.acs.org.

■ AUTHOR INFORMATION

Corresponding Author

*(D.C.) Tel: +39 55 4573722. Fax: +39 55 4573780. E-mail: daniela.catarzi@unifi.it. (S.M.) Tel: +39 049 8275704. Fax: +39 049 8275366. E-mail: stefano.moro@unipd.it.

■ ABBREVIATIONS USED

AR, adenosine receptor; cAMP, cyclic adenosine monophosphate; CGS21680, 2-[4-(2-carboxyethyl)phenethyl]amino-5′-(N-ethylcarboxamido)adenosine; CHA, N^6-cyclohexyladenosine; CHO, Chinese hamster ovary; DPCPX, 8-cyclopentyl-1,3-dipropyl-xanthine; EL2, second extracellular loop; GPCRs, G protein-coupled receptors; h, human; I-AB-MECA, N^6-(4-amino-3-iodobenzyl)-5′-(N-methylcarboxamido)adenosine; MOE, Molecular Operating Environment; NECA, 5′-(N-ethylcarboxamido)adenosine; rmsd, root-mean-square deviation; Ro20-1724, 4-(3-butoxy-4-methoxybenzyl)imidazolidin-2-one; SAR, structure—affinity relationship; TM, transmembrane; ZM-241385, 4-(2-[7-amino-2-(2-furyl)[1,2,4]-triazolo[2,3-a][1,3,5]triazin-5-ylamino]ethyl)phenol

■ REFERENCES

(1) Fredholm, B. B.; Ijzerman, A. P.; Jacobson, K. A.; Klotz, K. N.; Linden, J. International union of Pharmacology XXV. Nomenclature and classification of adenosine receptors. *Pharmacol. Rev.* **2001**, *53*, 527–552.

(2) Jacobson, K. A.; Knutsen, L. J. S. P1 and P2 purine and pyrimidine receptor ligands. In *Purinergic and Pyrimidinergic Signalling*; Abbracchio, M. P., Williams, M., Eds; Springer: Berlin, 2001; Handbook of Experimental Pharmacology, Vol. 151/1, pp 129–175.

(3) Abbracchio, M. P.; Brambilla, R.; Kim, H. O.; von Lubitz, D. K. J. E.; Jacobson, K. A.; Cattabeni, F. G-protein-dependent activation of phospholipase-C by adenosine A_3 receptor in rat brain. *Mol. Pharmacol.* **1995**, *48*, 1083–1045.

(4) Shneyvays, V.; Leshem, D.; Zinman, T.; Mamedova, L. K.; Jacobson, K. A.; Shainberg, A. Role of adenosine A_1 and A_3 receptors in regulation of cardiomyocyte homeostasis after mitochondrial respiratory chain injury. *Am. J. Physiol. Heart Circ. Physiol.* **2005**, *288*, H2792–H2801.

(5) Schulte, G.; Fredholm, B. B. Signalling from adenosine receptors to mitogen-activated protein kinases. *Cell. Signalling* **2003**, *15*, 813–827.

(6) Cunha, R. A. Adenosine ad a neuromodulator and as a homeostatic regulator in the nervous system: Different roles, different sources and different receptors. *Neurochem. Int.* **2001**, *38*, 107–125.

(7) Pedata, F.; Pugliese, A. M.; Coppi, E.; Popoli, P.; Morelli, M.; Schwarzschild, M. A.; Melani, A. adenosine in the central nervous system: Effects on neurotransmission and neuroprotection. *Immunol., Endocr. Metab. Agents Med. Chem.* **2007**, *7*, 304–321.

(8) Ribeiro, J. A. What can adenosine neuromodulation do for neuroprotection?. *Curr. Drug Targets: CNS Neurol. Disord.* **2005**, *4*, 325–329.

(9) Brambilla, R.; Cattabeni, F.; Ceruti, S.; Barbieri, D.; Franceschi, C.; Kim, Y-C; Jacobson, K. A.; Klotz, K.-N; Lohse, M. J.; Abbracchio, M. P. Activation of the A_3 adenosine receptor affect cell cycle progression and cell growth. *Naunyn-Schmiedeberg's Arch. Pharmacol.* **2000**, *361*, 225–234.

(10) Pugliese, A. M.; Coppi, E.; Spalluto, G.; Corradetti, R.; Pedata, F. A_3 adenosine receptor antagonists delay irreversible synaptic failure caused by oxigen and glucose deprivation in the rat CA1 hippocampus in vitro. *Br. J. Pharmacol.* **2006**, *147*, 524–532.

(11) Pugliese, A. M.; Coppi, E.; Volpini, R.; Cristalli, G.; Corradetti, R.; Jeong, L. S.; Jacobson, K. A.; Pedata, F. Role of adenosine A_3 receptors on CA1 hippocampal neurotransmission during oxygen-glucose deprivation episodes of different duration. *Biochem. Pharmacol.* **2007**, *74*, 768–779.

(12) Colotta, V.; Catarzi, D.; Varano, F.; Capelli, F.; Lenzi, O.; Filacchioni, G.; Martini, C.; Trincavelli, L.; Ciampi, O.; Pugliese, A. M.; Pedata, F.; Schiesaro, A.; Morizzo, E.; Moro, S. New 2-arylpyrazolo[3,4-c]quinoline derivatives as potent and selective human A_3 adenosine receptor antagonists: Synthesis, pharmacological evaluation, and ligand-receptor modeling studies. *J. Med. Chem.* **2007**, *50*, 4061–4074.

(13) Gessi, S.; Merighi, S.; Varani, K.; Leung, E.; Mac Lennan, S.; Borea, P. A. The A_3 adenosine receptor: An enigmatic player in cell biology. *Pharmacol. Ther.* **2008**, *117*, 123–140.

(14) Merighi, S.; Mirandola, P.; Varani, K.; Gessi, S.; Leung, E.; Baraldi, P. G.; Tabrizi, M. A.; Borea, P. A. A glance at adenosine receptors: A novel target for antitumor therapy. *Pharmacol. Ther.* **2003**, *100*, 31–48.

(15) Merighi, S.; Benini, A.; Mirandola, P.; Gessi, S.; Varani, K.; Leung, E.; Maclennan, S.; Borea, P. A. Adenosine modulates vascular endotelial growth factor expression via hypoxia-inducible factor-1 in human glioblastoma cells. *Biochem. Pharmacol.* **2006**, *72*, 19–31.

(16) Lee, H. T.; Ota-Setlik, A.; Xu, H.; D'Agati, V. D.; Jacobson, M. A.; Emala, C. W. A_3 adenosine receptor knockout mice are protected against ischemia- and myoglobinuria-induced renal failure. *Am. J. Physiol. Renal Physiol.* **2003**, *284*, 267–273.

(17) Yang, H.; Avila, M. Y.; Peterson-Yantorno, K.; Coca-Prados, M.; Stone, R. A.; Jacobson, K. A.; Civan, M. M. The cross-species A_3 adenosine receptor antagonist MRS 1292 inhibits adenosine-triggered human non pigmented ciliary epithelial cell fluid release and reduces mouse intraocular pressure. *Curr. Eye Res.* **2005**, *30*, 747–754.

(18) Colotta, V.; Catarzi, D.; Varano, F.; Cecchi, L.; Filacchioni, G.; Martini, C.; Trincavelli, L.; Lucacchini, A. 1,2,4-Triazolo[4,3-a]quinoxalin-1-one: A versatile tool for the synthesis of potent and selective adenosine receptor antagonists. *J. Med. Chem.* **2000**, *43*, 1158–1164.

(19) Colotta, V.; Catarzi, D.; Varano, F.; Cecchi, L.; Filacchioni, G.; Martini, C.; Trincavelli, L.; Lucacchini, A. Synthesis and structure-activity relationships of a new sets of 2-arylpyrazolo[3,4-c]quinoline derivatives as adenosine receptor antagonists. *J. Med. Chem.* **2000**, *43*, 3118–3124.

(20) Colotta, V.; Catarzi, D.; Varano, F; Filacchioni, G.; Martini, C.; Trincavelli, L.; Lucacchini, A. Synthesis and structure-activity relationships of a new set of 1,2,4-triazolo[4,3-a] quinoxalin-1-one derivatives as adenosine receptor antagonists. *Bioorg. Med. Chem.* **2003**, *11*, 3541–3550.

(21) Colotta, V.; Catarzi, D.; Varano, F.; Calabri, F. R.; Lenzi, O.; Filacchioni, G.; Trincavelli, L.; Martini, C.; Deflorian, F.; Moro, S. 1,2,4-Triazolo[4,3-a]quinoxalin-1-one moiety as an attractive scaffold to develop new potent and selective human A_3 adenosine receptor antagonists: synthesis, pharmacological and ligand-receptor modeling studies. *J. Med. Chem.* **2004**, *47*, 3580–3590.

(22) Catarzi, D.; Colotta, V.; Varano, F.; Calabri, F. R.; Lenzi, O.; Filacchioni, G.; Trincavelli, L.; Martini, C.; Tralli, A.; Montopoli, C.; Moro, S. 2-Aryl-8-chloro-1,2,4-triazolo[1,5-a]quinoxalin-4-amines as highly potent A_1 and A_3 adenosine receptor antagonists. *Bioorg. Med. Chem.* **2005**, *13*, 705–715.

(23) Catarzi, D.; Colotta, V.; Varano, F.; Lenzi, O.; Filacchioni, G.; Trincavelli, L.; Martini, C.; Montopoli, C.; Moro, S. 1,2,4-Triazolo[1,5-a]quinoxaline as a versatile tool for the design of selective human A_3 adenosine receptor antagonists: synthesis, biological evaluation and molecular modeling studies of 2-(hetero)aryl- and 2-carboxy-substituted derivatives. *J. Med. Chem.* **2005**, *48*, 7932–7945.

(24) Lenzi, O.; Colotta, V.; Catarzi, D.; Varano, F.; Filacchioni, G.; Martini, C.; Trincavelli, L.; Ciampi, O.; Varani, K.; Marighetti, F.; Morizzo, E.; Moro, S. 4-Amido-2-aryl-1,2,4-triazolo[4,3-a]quinoxalin-1-ones as new potent and selective human A_3 adenosine receptor antagonists. Synthesis, pharmacological evaluation and and ligand-receptor modeling studies. *J. Med. Chem.* **2006**, *49*, 3916–3925.

(25) Colotta, V.; Catarzi, D.; Varano, F.; Lenzi, O.; Filacchioni, G.; Martini, C.; Trincavelli, L.; Ciampi, O.; Traini, C.; Pugliese, A. M.; Pedata, F.; Morizzo, E.; Moro, S. Synthesis, ligand-receptor modeling studies and pharmacological evaluation of novel 4-modified 1,2,4-triazolo[4,3-a]quinoxalin-1-one derivatives as potent and selective human A$_3$ adenosine receptor antagonists. *Bioorg. Med. Chem.* **2008**, *16*, 6086–6102.

(26) Colotta, V.; Capelli, F.; Lenzi, O.; Catarzi, D.; Varano, F.; Poli, D.; Vincenzi, F.; Varani, K.; Borea, P. A.; Dal Ben, D.; Volpini, R.; Cristalli, G.; Filacchioni, G. Novel potent and highly selective human A$_3$ adenosine receptor antagonists belonging to the 4-amido-2-arylpyrazolo[3,4-c]quinoline series: Molecular docking analysis and pharmacological studies. *Bioorg. Med. Chem.* **2009**, *17*, 401–410.

(27) Colotta, V.; Lenzi, O.; Catarzi, D.; Varano, F.; Filacchioni, G.; Martini, C.; Trincavelli, L.; Ciampi, O.; Pugliese, A. M.; Traini, C.; Pedata, F.; Schiesaro, A.; Morizzo, E.; Moro, S. Pyrido[2,3-e]-1,2,4-triazolo[4,3-a]pyrazin-1-one as a new scaffold to develop potent and selective human A$_3$ adenosine receptor antagonists. Pharmacological evaluation, and ligand-receptor modeling studies. *J. Med. Chem.* **2009**, *52*, 2407–2419.

(28) Morizzo, E.; Capelli, F.; Lenzi, O.; Catarzi, D.; Varano, F.; Filacchioni, G.; Vincenzi, F.; Varani, K.; Borea, P. A.; Colotta, V.; Moro, S. Scouting human A$_3$ adenosine receptor antagonist binding mode using a molecular simplification approach: from triazoloquinoxaline to a pyrimidine skeleton as a key study. *J. Med. Chem.* **2007**, *50*, 6596–6606.

(29) Lenzi, O.; Colotta, V.; Catarzi, D.; Varano, F.; Poli, D.; Filacchioni, G.; Varani, K.; Vincenzi, F.; Borea, P. A.; Paoletta, S.; Morizzo, E.; Moro, S. 2-Phenylpyrazolo[4,3-d]pyrimidin-7-one as a new scaffold to obtain potent and selective human A$_3$ adenosine receptor antagonists: New insights into the receptor-antagonist recognition. *J. Med. Chem.* **2009**, *52*, 7640–7652.

(30) Biquard, D.; Grammaticakis, P. The absorption spectra of the phenylhydrazides of various diacids. II. Phenylhydrazides of phthalic acid. *Bull. Soc. Chim. France* **1942**, *5*, 675–689.

(31) Becker, D.; Botoshhansky, M.; Gasper, N.; Herbstein, F. H.; Karni, M. 2-Phenyl-4-hydroxyphthalazin-1-one: A benzoanellated derivative of maleic hydrazide. *Acta Crystallogr., Sect. B: Struct. Sci.* **1998**, *54*, 671–676.

(32) Drain, D. J.; Seymour, D. E. Some compounds related to 1,2-dihydro-4-hydroxy-1-oxo-2-phenylphthalazine. *J. Chem. Soc.* **1955**, 852–855.

(33) Jaakola, V. P.; Griffith, M. T.; Hanson, M. A.; Cherezov, V.; Chien, E. Y. T.; Lane, J. R.; Ijzerman, A. P.; Stevens, R. C. The 2.6 Angstrom Crystal Structure of a Human A$_{2A}$ Adenosine Receptor Bound to an Antagonist. *Science* **2008**, *322*, 1211–1217.

(34) Morizzo, E.; Federico, S.; Spalluto, G.; Moro, S. Human A$_3$ adenosine receptor as versatile G protein-coupled receptor example to validate the receptor homology modeling technology. *Curr. Pharm. Des.* **2009**, *15*, 4069–4084.

(35) Van der Muijlwik-Koezen, J. E.; Timmermann, H.; van der Goot, H.; Menge, W. M. P. B.; von Drabbe Künzel, J. F.; de Groote, M.; IJzerman, A. P. Isoquinoline and quinazoline urea analogues as antagonists for the human adenosine A$_3$ receptor. *J. Med. Chem.* **2000**, *43*, 2227–2238.

(36) Kim, J.; Wess, J.; van Rhee, M.; Schöneberg, T.; Jacobson, K. A. Site-directed mutagenesis identifies residues involved in ligand recognition in the human A$_{2A}$ adenosine receptor. *J. Biol. Chem.* **1995**, *270*, 13987–13997.

(37) Gao, Z.-G.; Chen, A.; Barak, D.; Kim, S.-K.; Müller, C. E.; Jacobson, K. A. Identification by site-directed mutagenesis of residues involved in ligand recognition and activation of the human A$_3$ adenosine receptor. *J. Biol. Chem.* **2002**, *277*, 19056–19063.

(38) Cheong, S. L.; Dolzhenko, A.; Kachler, S.; Paoletta, S.; Federico, S.; Cacciari, B.; Dolzhenko, A.; Klotz, K.-N.; Moro, S.; Spalluto, G.; Pastorin, G. The significance of 2-furyl Ring substitution with a 2-(para-substituted) aryl group in a new series of pyrazolo-triazolo-pyrimidines as potent and highly selective hA$_3$ adenosine receptors antagonists: New insights into structure-affinity relationship and receptor-antagonist recognition. *J. Med. Chem.* **2010**, *53*, 3361–3375.

(39) *MOE (Molecular Operating Environment)*, version 2009.10; Chemical Computing Group Inc.: Montreal, Quebec, Canada; http://www.chemcomp.com.

(40) Stewart, J. J. P. *MOPAC* 7; Fujitsu Limited: Tokyo, Japan, 1993.

(41) *GOLD suite*, version 1.3.2; Cambridge Crystallographic Data Centre: Cambridge, United Kingdom; http://www.ccdc.cam.ac.uk.

(42) Ballesteros, J. A.; Weinstein, H. Integrated methods for the construction of three dimensional models and computational probing of structure-function relationships in G-protein coupled receptors. *Methods Neurosci.* **1995**, *25*, 366–428.

(43) Labute, P. Protonate 3D: Assignment of ionization states and hydrogen coordinates to macromolecular structures. *Proteins* **2009**, *75*, 187–205.

(44) Halgren, T. A.; Myrphy, R. B.; Friesner, R. A.; Beard, H. S.; Frye, L. L.; Pollard, W. T. Glide: A new approach for rapid, accurate docking and scoring 1 methods and assessment of docking accuracy. *J. Med. Chem.* **2004**, *47*, 1739–1749.

(45) Korb, O.; Stützle, T.; Exner, T. E. Empirical Scoring Functions for advanced Protein-Ligand Docking with PLANTS. *J. Chem. Inf. Model.* **2009**, *49*, 84–96.

(46) Pastorin, G.; Federico, S.; Paoletta, S.; Corradino, M.; Cateni, F.; Cacciari, B.; Klotz, K.-N.; Gao, Z.-G.; Jacobson, K. A.; Spalluto, G.; Moro, S. Synthesis and pharmacological characterization of a new series of 5,7-disubstituted-[1,2,4]triazolo[1,5-a][1,3,5]triazine derivatives as adenosine receptor antagonists: A preliminary inspection of ligand-receptor recognition process. *Bioorg. Med. Chem.* **2010**, *18*, 2524–2536.

(47) Novellino, E.; Cosimelli, B.; Ehlardo, M.; Greco, G.; Iadanza, M.; Lavecchia, A.; Rimoli, M. G.; Sala, A.; Da Settimo, A.; Primofiore, G.; Da Settimo, F.; Taliani, S.; La Motta, C.; Klotz, K.-N.; Tuscano, D.; Trincavelli, M. L.; Martini, C. 2-(Benzimidazol-2-yl)quinoxalines: A novel class of selective antagonists at human A(1) and A(3) adenosine receptors designed by 3D database searching. *J. Med. Chem.* **2005**, *48*, 8253–8260.

(48) Nordstedt, C; Fredholm, B. A modification of a Protein-Binding Method for rapid quantification of cAMP in cell-culture supernatants and body fluid. *Anal. Biochem.* **1990**, *189*, 231–234.

(49) Cheng, Y. C.; Prusoff, W. H. Relation between the inhibition constant K$_i$ and the concentration of inhibitor which causes fifty percent inhibition (IC$_{50}$) of an enzyme reaction. *Biochem. Pharmacol.* **1973**, *22*, 3099–3108.